




Determination of the Basic Friction Angle of Rock Surfaces by Tilt Tests

Hyun-Sic Jang¹ · Qing-Zhao Zhang² · Seong-Seung Kang³ · Bo-An Jang¹ 

Received: 6 August 2017 / Accepted: 16 December 2017 / Published online: 28 December 2017
© Springer-Verlag GmbH Austria, part of Springer Nature 2017

Abstract

Samples of Hwangdeung granite from Korea and Berea sandstone from USA, both containing sliding planes, were prepared by saw-cutting or polishing using either #100 or #600 grinding powders. Their basic friction angles were measured by direct shear testing, triaxial compression testing, and tilt testing. The direct shear tests and triaxial compression tests on the saw-cut, #100, and #600 surfaces indicated that the most reliable results were obtained from the #100 surface: basic friction angle of 29.4° for granite and 34.1° for sandstone. To examine the effect of surface conditions on the friction angle in tilt tests, the sliding angles were measured 50 times with two surface conditions (surfaces cleaned and not cleaned after each measurement). The initial sliding angles were high regardless of rock type and surface conditions and decreased exponentially as measurements continued. The characteristics of the sliding angles, differences between tilt tests, and dispersion between measurements in each test indicated that #100 surface produced the most reliable basic friction angle measurement. Without cleaning the surfaces, the average angles for granite (32 measurements) and sandstone (23 measurements) were similar to the basic friction angle. When 20–50 measurements without cleaning were averaged, the basic friction angle was within $\pm 2^\circ$ for granite and $\pm 3^\circ$ for sandstone. Sliding angles using five different tilting speeds were measured but the average was similar, indicating that tilting speed (between 0.2° and 1.6°/s) has little effect on the sliding angle. Sliding angles using four different sample sizes were measured with the best results obtained for samples larger than 8 × 8 cm.

Keywords Basic friction angle · Direct shear test · Triaxial compression test · Tilt test · Hwangdeung granite · Berea sandstone

List of symbols

σ_n	Effective normal stress	β	Sliding angle
τ	Shear stress	l	Length of sample
c	Cohesion	h	Height of sample
ϕ	Friction angle	w	Width of sample
ϕ_b	Basic friction angle	UCS	Uniaxial compressive strength
d_n	Dilation components	V_p	P wave velocity
s_n	Shear component	σ_1	Axial stress
JRC	Joint roughness coefficient	σ_3	Confining pressure
JCS	Joint compressive strength	α	Angle of the pre-cut plane

✉ Bo-An Jang
bajang@kangwon.ac.kr

¹ Department of Geophysics, Kangwon National University, Kangwondaehakgil, Chuncheon, Gangwon-do 24341, Republic of Korea

² Department of Geotechnical Engineering, College of Civil Engineering, Tongji University, Shanghai 200092, SH, China

³ Department of Energy and Resource Engineering, Chosun University, 309 Pilmun-daero Dong-Gu, Gangju, Republic of Korea

1 Introduction

The engineering properties of rock masses are strongly influenced by the shear behavior of the joints because their shear strength is much lower than that of intact rock. The main factors affecting the shear strength of an unfilled joint are the rock type, the magnitude of the normal stress on the joint, the roughness and size of the joint, the degree of weathering, the joint wall strength, moisture, and water pressure. However, in a filled joint the mechanical properties of the filling

material dominate the shear strength of the joint (Kulatilake et al. 1995). It is very difficult to theoretically establish the joint shear strength criterion because natural rock joints are very diverse and complex; therefore, researchers have presented various empirically derived shear strength criteria rather than theoretical ones (Patton 1966; Goldstein et al. 1966; Ladanyi and Archambault 1969; Barton and Choubey 1977; Maksimovic 1992; Kulatilake et al. 1995; Papaliangas et al. 1995; Grasselli and Egger 2003; Jang and Jang 2015). In early studies on the shear strength of joints, the effective normal stress (σ_n) and shear strength (τ) were explained by the linear relation $\tau = c + \sigma_n \tan \phi$. The friction angle (ϕ) is the sum of the dilation angle determined by the roughness of the joint and the basic friction angle (ϕ_b) of the rock. At low normal stresses, the shear strength is affected only by the friction angle without cohesion (Newland and Allely 1957). When the normal stress is high, the asperities are destroyed. The shear strength can be expressed by the residual friction angle and apparent cohesion. The relation between the shear strength and the normal stress for a wide range of normal stresses can be expressed as a bilinear relation (Patton 1966; Goldstein et al. 1966).

Even before the linear shear strength criterion was suggested, many researchers knew that the relation between the normal stress and shear strength was nonlinear as a result of asperity destruction (Jaeger 1959; Krsmanovic and Langog 1964; Lane and Heck 1964; Patton 1966; Byerlee 1967; Ladanyi and Archambault 1969; Barton 1973). The most well-known nonlinear shear strength relation is the equation suggested by Barton (1973) and Barton and Choubey (1977). Barton (1973) explained the concept of the total friction angle of a joint as the sum of the basic friction angle (ϕ_b), the dilation components related to asperity angles (d_n), and the shear component related to the destruction of the asperity (s_n). He suggested a shear strength equation ($\tau = \sigma_n \tan[JRC \log(JCS/\sigma_n) + \phi_b]$) in which ' $d_n + s_n$ ' is described by a function of the joint roughness coefficient (JRC), joint compressive strength (JCS), and normal stress (σ_n). Barton and Choubey (1977) suggested that the residual friction angle may be used instead of ϕ_b in weathered or altered joints. Many researchers modified the equation presented by Barton and Choubey (1977) by quantitatively determining the JRC (Reeves 1985; Kulatilake et al. 1995; Grasselli and Egger 2003; Jang et al. 2010). Since the beginning of the twenty-first century, the characteristics of rock joints have been quantified very precisely with the shear strength of joints calculated based on three-dimensional roughness descriptions (Belem et al. 2000; Yang and Chiang 2000; Grasselli et al. 2002; Park and Song 2013; Jang and Jang 2015). It should be noted that most of the proposed joint shear strength relationships include the joint roughness and basic friction angles, indicating the importance of these two factors for calculating the shear strength. Thus,

they must be accurately measured to accurately predict the shear strength of the joints. Many researchers have tried to quantitatively determine the roughness of irregular and complicated joints; however, the basic friction angle has not been thoroughly studied because of the notion that the basic friction angle can be measured easily and simply. Most studies that examined basic friction angles used only the result of tilt tests (Horn and Deere 1962; Stimpson 1981; Cruden and Hu 1988; Bruce et al. 1989; Wines and Lilly 2003; Alejano et al. 2012; Ruiz and Li 2014; González et al. 2014).

The basic friction angle is the friction angle measured on a flat surface and is an intrinsic property of the rock, determined by the mineral composition and texture of the material (Patton 1966; Barton 1973). Barton (1973, 1976) compiled the basic friction angles of various rock types and reported a friction angle range of 21°–38°. The basic friction angles measured on sedimentary rocks ranged from 25° to 30° and those on igneous and metamorphic rocks ranged from 30° to 35°, indicating that sedimentary rock has a lower basic friction angle than other types of rock (Alejano et al. 2012). No standard method for testing the basic friction angle measurement has been suggested yet, but it is generally understood that a direct shear test on a flat surface yields the most accurate value. The values can also be obtained by triaxial compression tests using specimens with an inclined pre-cut plane and tilt tests. Direct shear tests and triaxial compression tests are more difficult to perform compared with tilt tests but yield relatively accurate results. The tilt test estimates the basic friction angle by measuring the angle when the tilted sample slides. This method is simple and easily applied, and thus, it is commonly used for basic friction angle measurements. Saw-cut surfaces or sand-blasted surfaces are used for most measurements. However, if very smooth surfaces are used in direct shear tests and triaxial compression tests, it is difficult to obtain accurate values because of stick–slip motion or because the shear stress increases continuously as the shear displacement increases (Barton 1973; Stimpson 1981). Other researchers compared the basic friction angle measured by direct shear testing with that measured by a tilt test. They found that the basic friction angle measured by the direct shear test is lower than that measured by the tilt test because small asperities wear out during shearing. Their results suggest that the planes should be completely polished to obtain a reliable value (Coulson 1970; Wines and Lilly 2003; Ruiz and Li 2014).

In recent years, basic friction angles have been measured mainly by using tilt tests for various types of samples as shown in Fig. 1 (Horn and Deere 1962; Stimpson 1981; Cruden and Hu 1988; Bruce et al. 1989; Wines and Lilly 2003; Alejano et al. 2012; Ruiz and Li 2014; González et al. 2014). A detailed study of the tilt test was first carried out by Stimpson (1981) who measured the sliding angle (β) with one core sample placed on two cores placed side

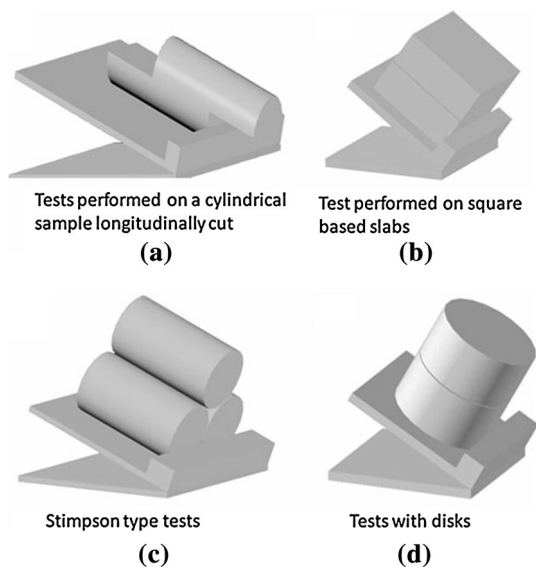


Fig. 1 Different setups for tilt tests (Alejano et al. 2012)

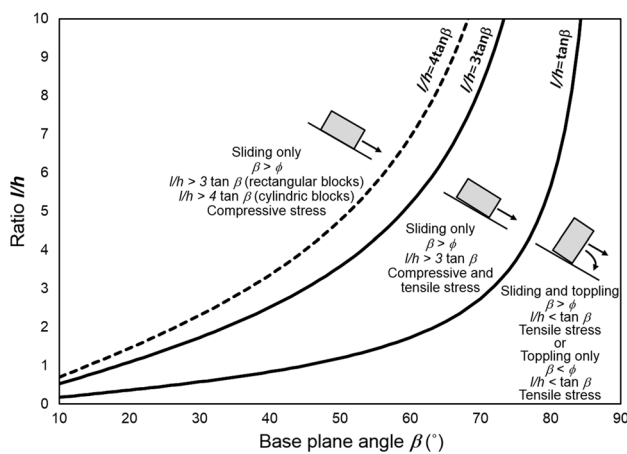


Fig. 2 Theoretical conditions ensuring full stress compressive contact between the sliding plane and the sliding slab (Alejano et al. 2012)

by side as shown in Fig. 1c. Stimpson proposed an equation to calculate the basic friction angle from the sliding angle ($\theta_b = \tan^{-1}(1.155 \tan \beta)$) using the limit equilibrium theory, which is not correct (González et al. 2014; Ruiz and Li 2014).

However, Alejano et al. (2012) noted that the basic friction angles obtained by Stimpson (1981) were somewhat higher than those collected by Barton (1973, 1976). Alejano et al. (2012) conducted tilt tests with four types of specimens as in Fig. 1 and compared the results to deduce the most appropriate way to obtain accurate basic friction angles. They also calculated the normal stress on the slip surface depending on the shapes of the samples and showed which shapes can slide without toppling (Fig. 2). In Fig. 2, l is the

length of the specimen, h is the height of the specimen, β is the sliding angle, and ϕ is the friction angle of the sliding face. Their results indicated that for rectangular blocks (as shown in Fig. 1b), the condition for sliding is $l/h \geq 3 \tan \beta$.

However, in most studies, including Stimpson (1981) and Alejano et al. (2012), the basic friction angles measured by tilt tests were often not normally distributed. The uncertainty of these results is thought to be caused by various factors that were not taken into consideration, such as the flatness of the surface of the sample, the polishing condition, irregularity of the tilting speed, vacuum adsorption, and the static electricity effect on the contact surface. Therefore, it is necessary to conduct a more detailed study of basic friction angle tilt tests to reduce the uncertainty of the test.

In this study, samples of Hwangdeung granite from Korea and Berea sandstone from the USA, both containing sliding planes, were prepared by saw-cutting or polishing using either #100 or #600 grinding powders. Their basic friction angles were then measured by direct shear tests and triaxial compression tests. The sliding angles were then measured by tilt tests on the same samples. The characteristics of the sliding angles in relation to the conditions of the sliding surfaces were statistically analyzed to determine the testing method that produced the most reliable measurements of the basic friction angle through tilt testing. The effects of the tilting speed and sample size in determining the basic friction angle were also examined.

2 Sample Preparation

Hwangdeung granite from Korea and the Berea sandstone from USA were used to prepare test samples (Fig. 3). Hwangdeung granite is medium-grained with a grain size of approximately 0.6–2.0 mm. It consists of quartz, plagioclase, K-feldspar, and biotite. Berea sandstone has a particle size of 0.1–0.8 mm, and feldspar and kaolin are the main minerals (Dehler and Labuz 2007). The density, porosity, uniaxial compressive strength, P wave velocity, Young’s modulus, and Poisson’s ratio for both samples were measured using the test methods suggested by the International Rock Mechanics Association (ISRM) (Table 1). The Hwangdeung granite was classified as a brittle rock of low porosity and high strength with a density of 2.63 g/cm³, porosity of 0.52%, uniaxial compressive strength of 184 MPa, and Young’s modulus of 57 GPa. The Berea sandstone is a relatively soft rock with a density of 2.20 g/cm³, porosity of 14.8%, uniaxial compressive strength of 79 MPa, and Young’s modulus of 20 GPa. The porosity of the Berea sandstone is 30 times greater than that of the granite, and the strength and Young’s modulus are less than half.

The samples used for the tilt tests and the direct shear tests were slabs with a length (l) of 10 cm, a width (w) of

10 cm, and a thickness (h) of 2 cm (Fig. 4a). The samples thus satisfy the condition of $l/h \geq 3 \tan \beta$, which is a normal slip condition below the sliding angle (β) of 59° (Alejano et al. 2012). For the triaxial compression test, a core sample with a diameter of 5.4 cm and a height of 11 cm with an inclined pre-cut plane at the middle portion was used. The angles between the normals to the pre-cut planes and the core axis were 40° , 50° , and 60° (Fig. 4b).

Three types of sliding surfaces were prepared to examine the effect of the different conditions of the sliding surface on the sliding angle. The first type of surface was cut by a diamond saw, a method commonly used in previous studies (Horn and Deere 1962; Stimpson 1981; Cruden and Hu 1988; Bruce et al. 1989; Grasselli and Egger 2003; Alejano et al. 2012). The saw-cut surface is almost flat

and smoothly polished by a high-speed rotating saw blade, although step-like cutting traces due to the saw blade are visible. To prepare the second and third types, the surfaces were polished by #100 and #600 grinding powder (hereafter referred as #100 surface and #600 surface). The #100 surface is flat and smooth, while the #600 surface is flatter and smoother than #100 surface and the saw-cut surface; however, it is not shiny like a mirror.

Six samples from the two types of rocks (Hwangdeung granite and Berea sandstone) and three types of surfaces (saw-cut, #100 surface, and #600 surface) were prepared for the direct shear test and the tilt test. Eighteen samples were prepared with the two types of rocks, three types of surfaces, and three types of pre-cut inclinations (40° , 50° , and 60°) for the triaxial compression test.

Fig. 3 Samples used for tilt tests and direct shear tests: **a** Hwangdeung granite, **b** Berea sandstone

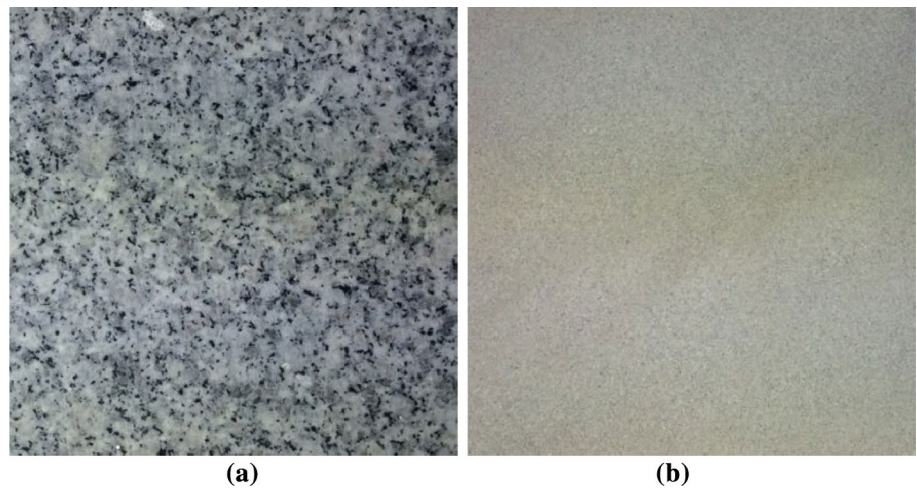
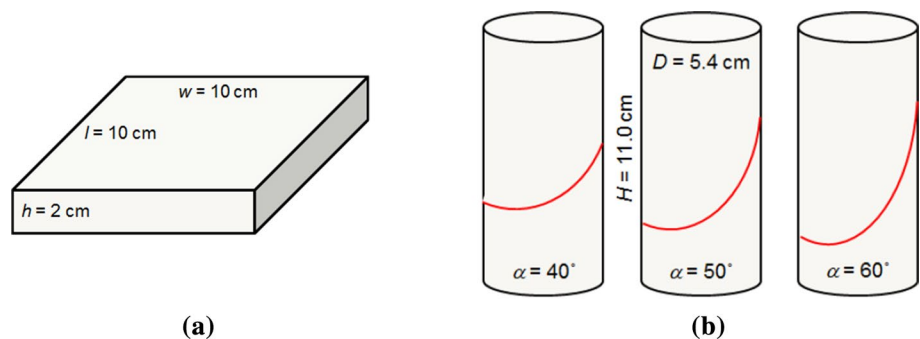


Table 1 Physical properties of the Hwangdeung granite and Berea sandstone

Rock type	Density (g/cm ³)	Porosity (%)	UCS (MPa)	V_p (m/s)	Young's modulus (GPa)	Poisson's ratio
Granite	2.63	0.52	183.9	3957	57.48	0.28
Sandstone	2.20	14.77	79.2	2650	20.49	0.33

UCS uniaxial compressive strength

Fig. 4 Shapes of samples used for **a** tilt test and direct shear test, **b** triaxial compression test. D and H are the diameter and height of the core samples, respectively. α is the angle between the normal to the pre-cut plane and the core axis



3 Determining the Basic Friction Angle

3.1 The Direct Shear Test

The direct shear tests were performed using the standard test method suggested by ISRM using an RM 102 Direct Shear Machine manufactured by SBEL, Phoenix, AZ, USA. This machine was originally designed to apply normal stress and shear stress by a manual hydraulic pump and subsequently modified to include an electric hydraulic pump, piston cylinder, loading frame, and hydraulic control device. Hydraulic pressure sensors and displacement gauges were installed to accurately control and measure the shear force, vertical force, shear displacement, and vertical displacement. The shear displacement rate was set at a slow speed of 0.1 mm/min to prevent stick–slip during the shear test. Six levels of vertical stresses from 0.5 MPa to 4.0 MPa were applied. Samples with #100 and #600 surfaces were re-polished at the end of each test to maintain consistent surface conditions. However, since the saw-cut surface cannot be reproduced, the dust and abraded rock particles generated during the shearing process were removed using a brush and compressed air at the end of each test.

The shear stress increased linearly as the shear displacement increased up to a certain displacement, and then the slope of the shear stress curves gradually decreased, reaching a constant level as a residual shear stress (Fig. 5). The peak shear stress was not observed because the surfaces were smooth without any roughness. In the surface #600 samples, the residual shear stress increased but then decreased suddenly, showing stick–slip behavior. Such stick–slip occurs on a very smooth surface because the shear forces accumulate as strain energy on the contact surface during the shear displacement and are suddenly released (Bridgman 1936; Brace and Byerlee 1966). The linear relationship between the shear stress and shear displacement σ_n represents

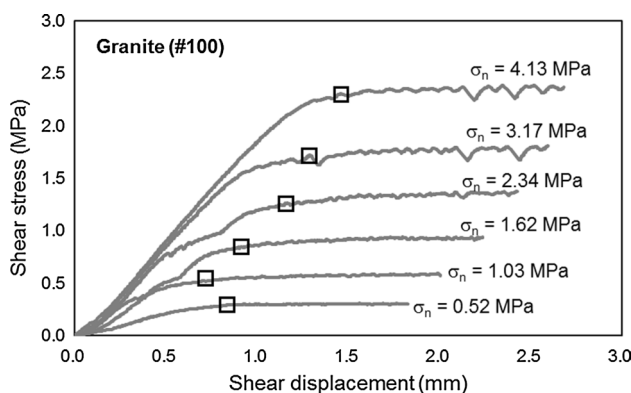


Fig. 5 Shear stresses measured during direct shear tests for granite samples polished using #100 grinding powder

the compressional deformation and/or shear deformation of the rock itself. Therefore, the shear stress at the point where the slope of the shear stress–shear displacement curve begins to decrease and stabilize, as shown by the squares in Fig. 5, is determined as the shear strength of the joint (Lee and Chang 2015).

The shear strength increases linearly with increasing normal stress (Fig. 6), unlike the nonlinear relationship between the normal stress and the peak shear strength for natural rough joints. This relationship is similar to that between the normal stress and the residual shear strength. All samples showed a very good linear correlation coefficient of 0.99 or more. The friction angle was obtained from the slope angle of the regression line. The friction angles of the granite were 29.2° for #100 surface, 28.6° for #600 surface, and 25.5° for the saw-cut surface (Fig. 6a). The difference between the values of the #100 surface and #600 surface was very small, only 0.6°; however, the friction angle of the saw-cut surface was 3° lower than that of the polished surfaces. The friction angles of the sandstone were 35.1° and 34.6° for #100 surface and the saw-cut surface, respectively, but was 8° lower (26.4°) for #600 surface. The sandstone showed more variability with the different surface conditions compared with the granite (Fig. 6b). The friction angles of the sandstone were 2°–9° larger than those of the granite.

3.2 Triaxial Compression Test

A 196-kN capacity compression machine (AceOne Tech., Ansan Korea) equipped with a servo control system and Hoek cell was used for the triaxial compression test. The inclined plane was pre-cut so that the shearing occurred along the pre-defined plane. When axial stress (σ_1) and confining pressure (σ_3) are applied to a specimen with a shear plane whose normal is inclined by α from the core axis (Fig. 7), the normal stress (σ_n) and shear stress (τ) in the plane can be obtained from Eqs. (1) and (2).

$$\sigma_n = \frac{\sigma_1 + \sigma_3}{2} + \frac{\sigma_1 - \sigma_3}{2} \cos 2\alpha \tag{1}$$

$$\tau = \frac{\sigma_1 - \sigma_3}{2} \sin 2\alpha \tag{2}$$

Five different confining pressures from 0.5 to 7 MPa were applied. The axial stress and displacement were measured until the shear displacement reached 4 mm. The axial stress was loaded by constant displacement control so that the shear displacement increased linearly. The loading speed was 0.1 mm/min, slower than the usual testing rate, to prevent stick slip. The triaxial compression tests were performed for samples with three different inclination angles (α) and five levels of confining pressures for each surface type. Each test was repeated twice to ensure reliability of the

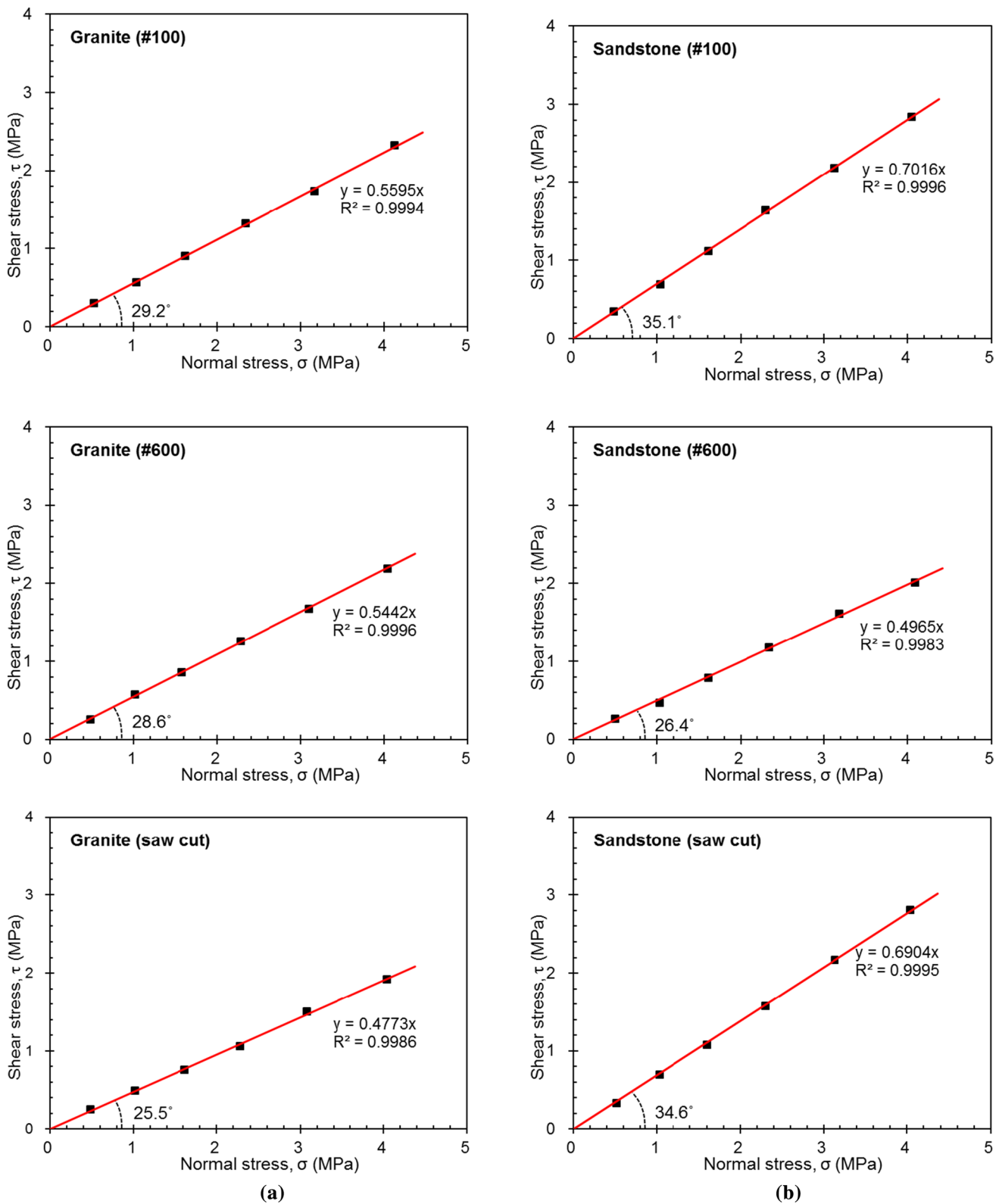


Fig. 6 Shear strengths with respect to normal stresses measured by direct shear tests for **a** granite and **b** sandstone cut by saw (labeled saw-cut) and polished using #100 and #600 grinding powders (labeled #100 and #600, respectively)

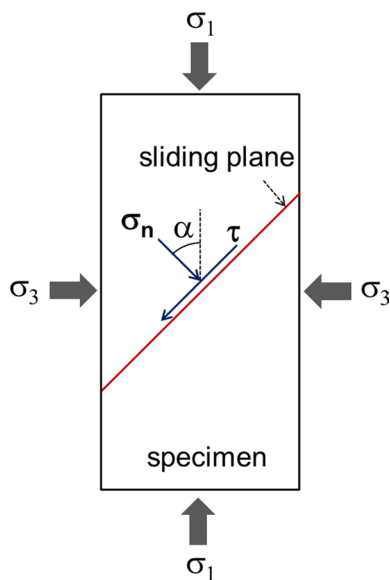


Fig. 7 Stress state on the sliding plane during triaxial compression test

test results. Surfaces #100 and #600 were re-polished after each test to maintain identical surface conditions for each sample. The saw-cut surface was cleaned with a brush and compressed air to remove dust particles and abraded rock particles from the surface.

As the shear displacement increased (Fig. 8), the shear stress increased almost linearly up to a certain point, then the gradient of the curve decreased gradually, and the shear stress reached an almost constant value as the residual stress without a peak shear stress. No stick–slip motion was observed, unlike the case of the direct shear test. The point where the shear stress became constant was considered as the shear strength. The shear stresses for the four samples

show a strong linear positive relation with the normal stresses (Fig. 9); the slope angles of the regression lines are the friction angles. The friction angles of the granite samples were 29.5° for #100 surface, 28.8° for #600 surface, and 25.2° for the saw-cut surface (Fig. 9a). The regression lines for the #100 and #600 surfaces show coefficients of determination (R^2) greater than 0.98, and the saw-cut surface also has a good linear relationship, with $R^2 > 0.97$. The friction angle measured on the saw-cut surface is 4° lower than those on the polished surfaces.

On the #100 surface and the saw-cut surface with $\alpha = 40^\circ$ in the sandstone samples, the axial stresses increased continuously without a peak as axial displacement increased during the triaxial compression test; therefore, the axial stresses when the actual shear displacement occurred could not be determined. This phenomenon may have occurred because α was too low compared with the friction angle of the rock. Therefore, the friction angle was calculated from the values measured in the samples with $\alpha = 50^\circ$ and 60° in the #100 surface and the saw-cut surface. The friction angles in the sandstone samples were 33.1° on #100 surface, 27.9° on #600 surface, and 32.3° on the saw-cut surface (Fig. 9b). The sandstone samples showed a linear relationship between the shear stress and the normal stress, with $R^2 > 0.99$ for the #100 and saw-cut surfaces and $R^2 = 0.98$ for #600 surface.

3.3 The Basic Friction Angle

The friction angles of the granite measured by direct shear tests and triaxial compression tests were consistent within 0.7° when measured on #100 and #600 surfaces and were approximately 4° lower when measured on the saw-cut surfaces. The friction angles of the sandstone measured by direct shear tests and triaxial compression tests were consistent within 0.8° with those measured on the #100 and saw-cut

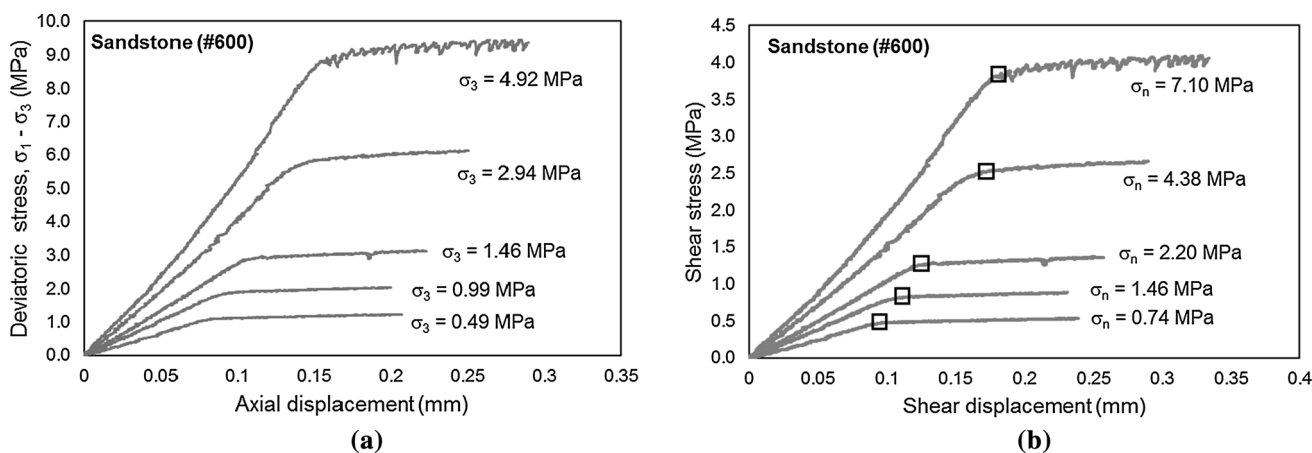


Fig. 8 a Deviatoric stress versus axial displacement curve and b shear stresses versus shear displacement curve in triaxial compression tests for sandstone samples polished using #600 grinding powder

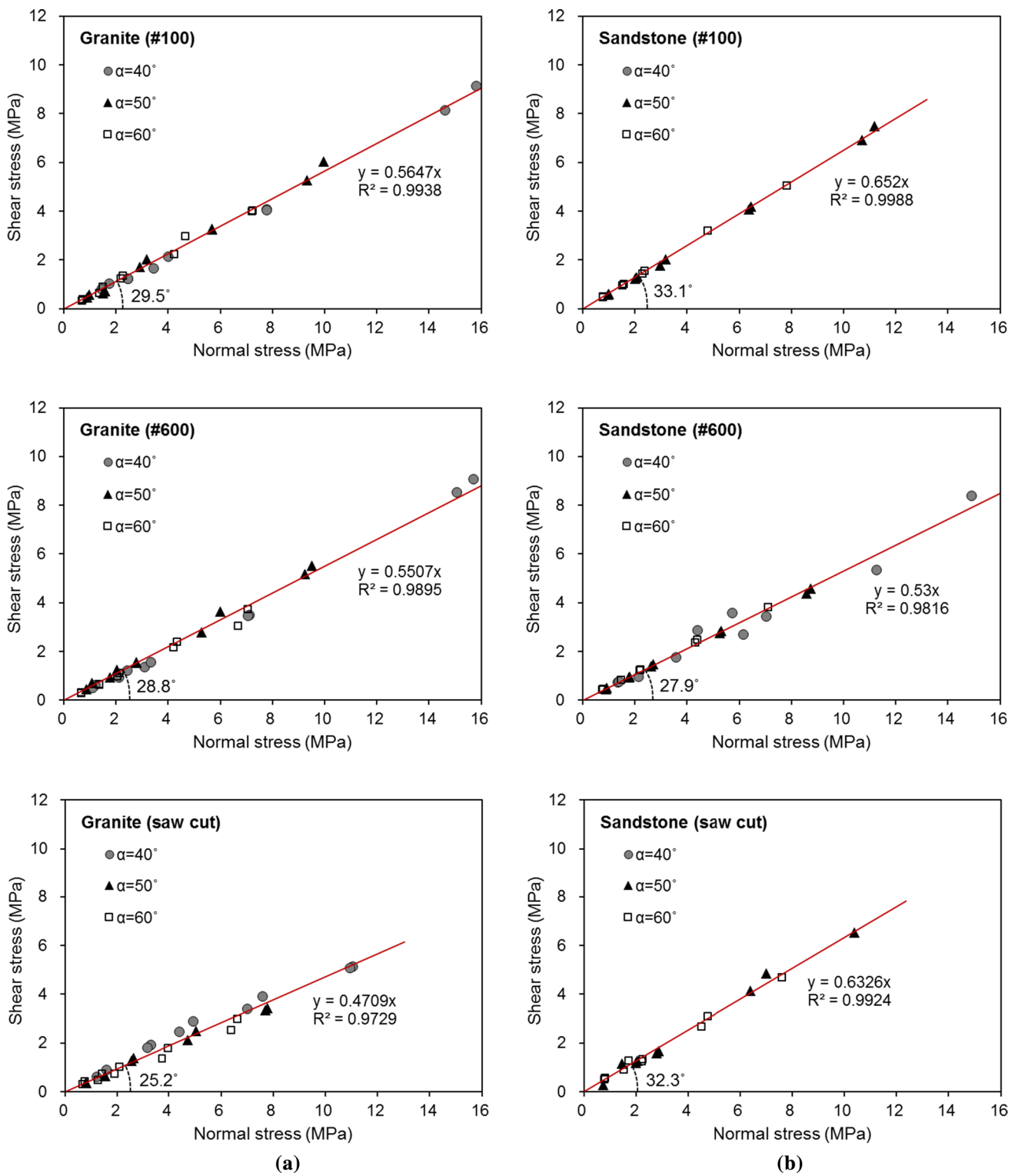


Fig. 9 Shear strengths with respect to normal stresses measured by triaxial compression tests for **a** granite and **b** sandstone. α is the angle of the pre-cut plane measured upward from the horizontal plane. The

labels #100 and #600 denote surfaces polished using #100 and #600 grinding powders, respectively

surfaces and were 5° – 8° smaller on the #600 surfaces. These results indicate that the measured friction angles may differ depending on the surface conditions within the same rock type. Note that the friction angle of the saw-cut surface in the granite samples and that of #600 surface in the sandstone are the lower for both rock types. The polished surfaces that were ground were very smooth and the two surfaces match almost completely while the smoothness of the saw-cut surfaces may vary depending on the samples, and two surfaces may not match perfectly in the shear test. The sandstone samples, which consist of relatively weak rock with low stiffness, are likely to come into close contact with each other because of the elastic deformation that develops when the normal stresses are applied. However, the granite samples, which are stronger and stiffer, are less likely to come into contact with each other when the normal stresses are applied. This may explain the small sliding angles of the saw-cut surface in the granite samples. Stick slip motion was widely observed in #600 surface of the sandstone sample during the direct shear test; this may be one reason for the low friction angle. Another reason may be that sliding was easier because of the very flat and smooth surface. All these results indicate that the most reliable measurements of the basic friction angle are obtained on #100 surface for both rock types. The average friction angle on #100 surface measured by direct shear test and triaxial compression test was calculated, and the basic friction angles of the granite and sandstone samples were determined as 29.4° and 34.1° , respectively.

The basic friction angles of granite and sandstone measured in this study are shown in Table 2 alongside the results of previous studies. The basic friction angle of the granite measured in this study is somewhat lower than that of Coulson (1972), but is similar to that of recent studies by Alejano et al. (2012) and González et al. (2014). The basic friction angle of the sandstone is approximately 2° larger than that found in the Krsmanovic (1967) study, but similar to the values measured by Patton (1966) and Coulson (1972).

Table 2 Comparison of basic friction angles determined by this study with previous studies

Rock type	Basic friction angles ($^{\circ}$)	References
Granite	31.0–35.0	Coulson (1972)
	26.2–39.6	Alejano et al. (2012)
	26.0–32.0	González et al. (2014)
	29.4	<i>This study</i>
Sandstone	26.0–35.0	Patton (1966)
	31.0–33.0	Krsmanovic (1967)
	32.0–34.0	Coulson (1972)
	34.1	<i>This study</i>

4 Tilt Test

The tilt test is the easiest and simplest method to estimate the basic friction angle from the sliding angle of the sample as shown in Fig. 1 (Horn and Deere 1962; Stimpson 1981; Cruden and Hu 1988; Bruce et al. 1989; Alejano et al. 2012; Jang and Jang 2015). However, a standard testing method has not yet been proposed. In this study, a tilt test using a slab sample (Fig. 4a) was performed following the method of Alejano et al. (2012). Tilt tests often use a simple testing apparatus that is manually operated. These testing systems cannot keep the tilting speed constant and cannot stop exactly when the upper block slips. To overcome these problems, recent studies used automated testing systems with electric motors (Alejano et al. 2012; Lee et al. 2014). In this study we used an automatic tilt tester manufactured by AceOne Tech. (Ansan, Korea) (Fig. 10). The apparatus has an electric motor system and a 20×20 cm tilt plate. The tilting speed can be adjusted from 0.2° to 1.8° per second. It can also detect the exact time of sliding and stop the tester using a laser motion detector. It has a digital slope meter (Disi-Pas DWL 80E) that can measure the sliding angle to 0.1° accuracy and an analog tiltmeter as an auxiliary meter. In this study, we set a tilting speed of about 0.4° per second so that the tilting speed did not affect the slip of the upper block (Alejano et al. 2012). The tilting device automatically stopped when the upper block placed on the fixed lower block slid more than 10 mm.

4.1 Characteristics of the Sliding Angles

In most tilt tests the sliding angle was measured repeatedly on a set of smooth surfaces, and then an average of the measured values was determined as the friction angle (Stimpson



Fig. 10 Photograph of the automated tilt test apparatus used in this study

1981; Cruden and Hu 1988; Muralha 1995; Alejano et al. 2012; González et al. 2014; Jang and Jang 2015). In this study, the sliding angles of the samples were measured 50 times and the variation of the angles with testing conditions was investigated. To examine the effect of cleaning the surface on the friction angle, two surface conditions—surfaces cleaned and not cleaned after each tilt measurement—were tested. The sliding surfaces were cleaned using a soft brush to remove abraded rock particles. #100 and #600 surfaces were re-polished after fifty measurements. These test procedures were repeated three times to ensure the reliability of the test. Because the initial condition of the saw-cut surface cannot be reproduced after the test, the sliding surfaces were only cleaned by a soft brush and compressed air between tests.

Figure 11 shows the tilt test results for the granite samples. The initial sliding angles of #100 and #600 surfaces are 37° – 40° , which are 8° – 11° higher than the basic friction angle measured in the direct shear test and triaxial compression test (around 29°). The sliding angle decreased exponentially as the measurements continued. The sliding angle at the 50th measurement for the #100 surfaces was about 23° when the surfaces were not cleaned and about 18° when the surfaces were cleaned, which is much lower than the basic friction angle from the other tests (Fig. 11a). The average sliding angle from 50 measurements was 27.6° when the surfaces were not cleaned and 23.5° when the surfaces were cleaned. These values are lower than the basic friction angle. The sliding angles of the last measurement for the #600 surfaces were approximately 19° when not cleaned and approximately 15° when cleaned (Fig. 11b). The averages of sliding angles from 50 measurements were 21.5° when the surfaces were not cleaned and 19.1° when the surfaces were cleaned. These values are also much lower than the basic friction angle. The sliding angles for the saw-cut surfaces show a different trend as the measurements proceed compared with the polished surfaces. They tend to increase or decrease linearly, but the differences between the measurements are very large (Fig. 11c). These results indicate that the sliding angles decrease more rapidly when the sliding surfaces were cleaned. The dispersion of the measurements in each test and the differences between the tests were the smallest when the sliding angles were measured using #100 surface without cleaning.

The trend of the sliding angle measurements for the sandstone samples was similar to those of granite on #100 and the saw-cut surfaces but different from the granite measurements on #600 surface (Fig. 12). The sliding angles measured on the #100 sandstone surfaces ranged from 42.4° to 27.2° when the surfaces were not cleaned and from 42.1° to 22.1° when the surfaces were cleaned. The angles decreased exponentially as the measurements continued and decreased more rapidly when the sliding surfaces were cleaned, similarly

to the granite curves. The average sliding angles of fifty measurements were 31.0° when not cleaned and 28.2° when cleaned (Fig. 12a). The differences between the averages of the sliding angles and the basic friction angle measured by the direct shear test and triaxial compression test were less than 3° when the surfaces were not cleaned. When the surfaces were not cleaned, the initial slip angles of the #600 surface were very low (23°) and increased as the measurements continued. However, when surfaces were cleaned they decreased very rapidly during the first few measurements and then very slowly (Fig. 12b). The averages of the sliding angles were 26.9° when not cleaned and 21.9° when cleaned. These values are much lower than the basic friction angle derived from the direct shear and triaxial tests. The variations between the tests were also large when the surfaces were not cleaned. These results indicate that the sliding angles measured on the #600 surface are not reliable. The sliding angles for the saw-cut surface were similar to those of the granite. The dispersion between the saw-cut surface measurements in each test and the differences between the tests were very large (Fig. 12c). The characteristics of the sliding angles, the differences within each tilt test, and the dispersion between measurements in each test indicate that the most reliable tilt test measurement of the basic friction angle is on #100 surface, as is the case in the direct shear test and triaxial compression test.

When the two surfaces were polished, no preferred sliding direction was produced because the surface was polished along a random direction. That is the reason for the high sliding angles observed in the first few tilt tests. As the measurements continued, the sliding surfaces were abraded to form a plane that became progressively easier to slide along, and the sliding angles became smaller. Although newly polished surfaces were used in the direct shear test and triaxial compression test, the friction angle was very consistent. In the direct shear test and triaxial compression test, high normal stress was applied at the surface; thus, the sliding was controlled only by the shear stress. However, in the tilt test very low normal stress was applied; thus, the surface condition and abrasion had a strong influence on the sliding angle.

Hencher (1976, 2012) reported that the slip angles for saw-cut surfaces of sandstone decreased from 30° to 10° when the surface was cleaned, but increased to 25° as the tests continued when the surface was not cleaned. González et al. (2014) also performed 300 tilt tests using three different saw-cut rock samples, such as gneiss, migmatite, and dunite, and reported similar results. In this study, the same tendency was observed when the sliding surfaces were cleaned. However, when the surfaces were not cleaned, the slip angle of #100 and #600 surfaces in the granite surfaces and #100 surfaces in the sandstone samples decreased and those of the saw-cut surfaces increased or decreased linearly as the measurement continued, unlike the results of Hencher

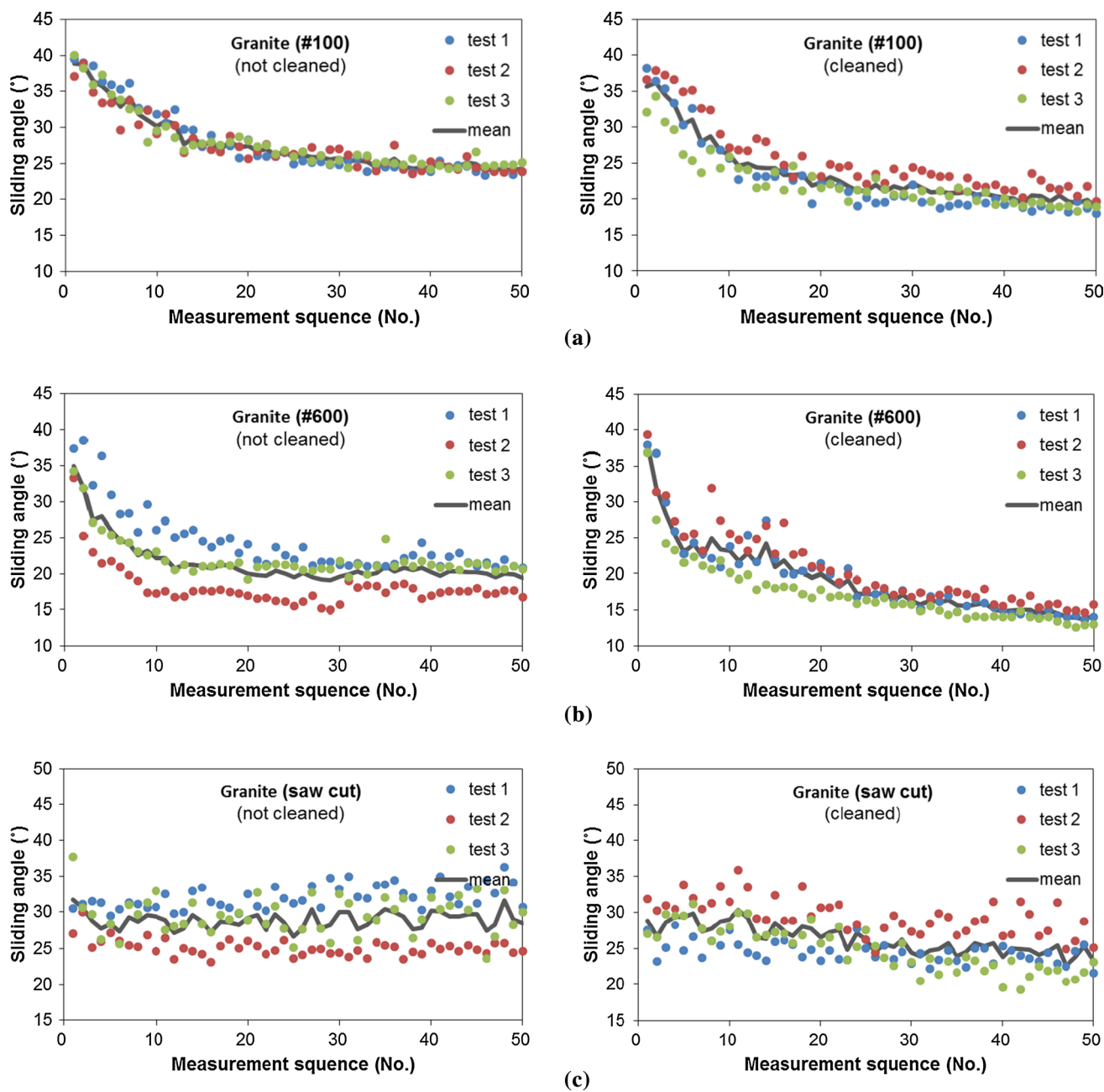


Fig. 11 Results of tilt tests for granite; the sliding surface was cleaned or not cleaned after each measurement. **a** #100 surface, **b** #600 surface, **c** saw-cut surface

(1976, 2012) and González et al. (2014). This indicates that the effect of cleaning the abraded rock particles between tests may differ depending on the strength and surface conditions of the rock.

Because the sliding angles for the newly polished surfaces were higher and those for the surfaces after a few tens of measurements were lower than the basic friction angle determined by the direct shear test and triaxial compression test, the optimal number of measurements was estimated by calculating the averages of the sliding angles

on the #100 surfaces at 10, 20, 30, 40, and 50 measurements (Table 3). The smaller the numbers of measurements, the higher the average values are. The sliding angle of the granite samples without cleaning was 34.4° when the first 10 measurements were averaged but 27.6° when 50 measurements were averaged. When the surface was cleaned, the averages of the first 10 and 50 measurements were 31.1° and 23.5°, respectively. The averages of 32 measurements without cleaning and 14 measurements with cleaning were very close to the basic friction angle

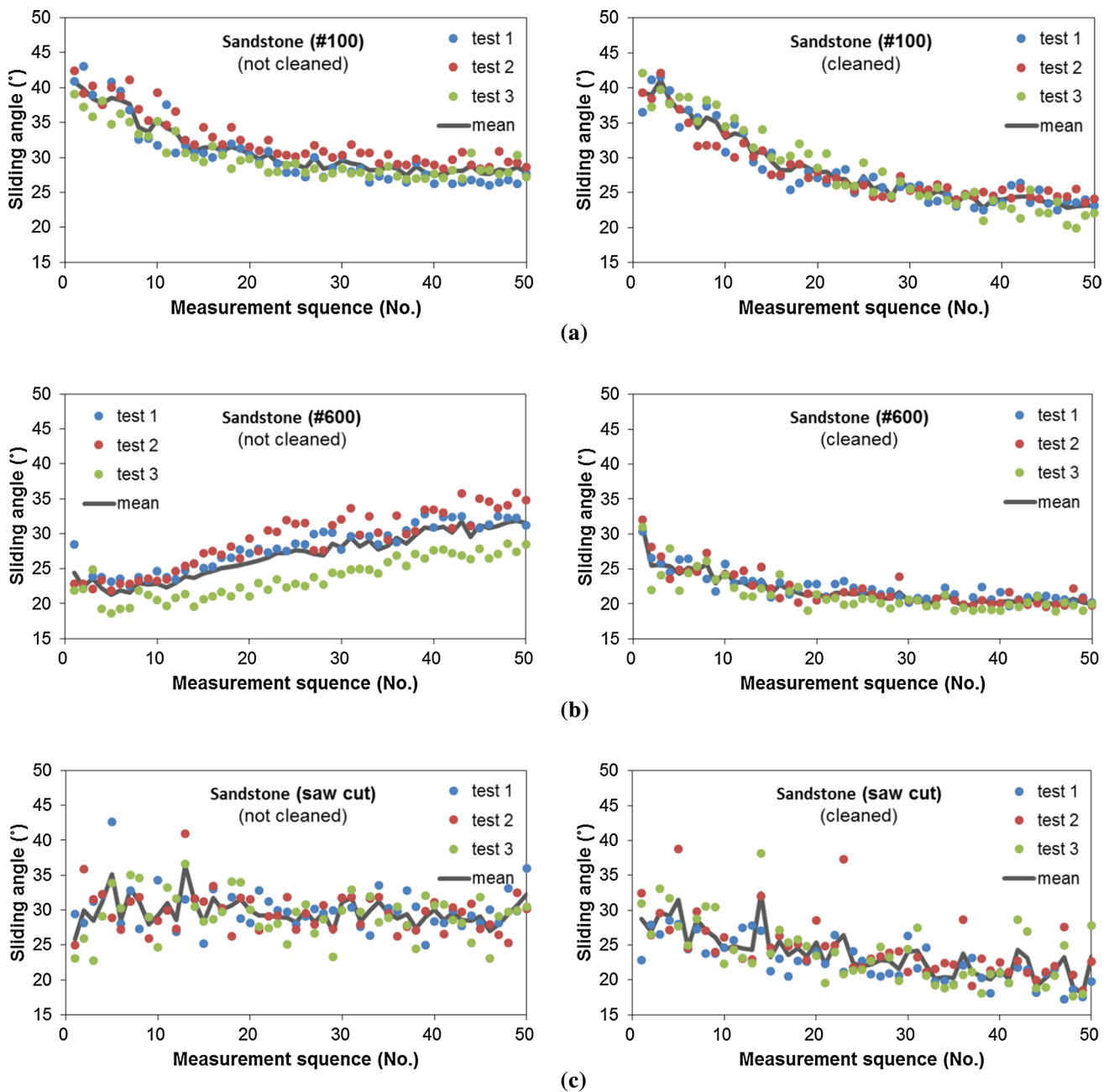


Fig. 12 Results of tilt tests for sandstone; the sliding surface was cleaned or not cleaned after each measurement. **a** #100 surface, **b** #600 surface, **c** saw-cut surface

of granite. In the sandstone samples, the average of the first 10 and 50 measurements was 37.4° and 31.0° without cleaning, and 36.9° and 28.2° with cleaning, respectively (Fig. 13). The averages of 23 measurements without cleaning and 18 measurements with cleaning were the same as the basic friction angle. The sliding angles decreased more rapidly when the surfaces were cleaned. The number of measurements used to estimate the basic friction angles was larger for both rock types when the sliding surfaces were not cleaned. The difference between the basic friction

angle and the sliding angle averaged over 50 measurements was 1.8° for the granite and 3.1° for the sandstone samples. The average of the first 20 measurements for the granite was 31.3° , which is 1.9° larger than the basic friction angle. The average of the first 20 measurements for the sandstone was 34.6° , which is 0.5° larger than the basic friction angle. This indicates that the basic friction angle can be measured within $\pm 2^\circ$ for granite and within $\pm 3^\circ$ for sandstone when 20–50 measurements without cleaning are averaged.

Table 3 Averages of sliding angles depending on numbers of measurements when sliding surface was cleaned or not cleaned

Rock type	Number of measurements	Average sliding angle	
		Not cleaned (°)	Cleaned (°)
Granite	10	34.4	31.1
	20	31.3	27.4
	30	29.6	25.5
	40	28.4	24.4
	50	27.6	23.5
Sandstone	10	37.4	36.9
	20	34.6	33.5
	30	32.8	31.1
	40	31.7	29.4
	50	31.0	28.2

In this research, the basic friction angle (ϕ_b) is determined by the average of friction angles measured during tilt tests. The average of friction angles is also calculated using the average of friction coefficients which are equal to $\tan \phi_b$. It seems that the latter method looks more correct. However, the differences of the basic friction angle between these two methods are very small, which is about 0.2° . This indicates that the basic friction angle can be measured by both methods.

4.2 Effect of Tilting Speed and Sample Size on the Sliding Angle

4.2.1 Effect of Tilting Speed

The tilting speed may affect the sliding angles; different tilting speeds may cause higher or lower sliding angles. The tilting speeds can be adjusted in the tilt test apparatus used in these experiments (Fig. 10); thus, five different tilting speeds of $0.2^\circ/s$, $0.4^\circ/s$, $0.8^\circ/s$, $1.2^\circ/s$, and $1.6^\circ/s$ were used

to investigate the effect of the tilting speed on the sliding angle. Based on the results presented above, only one granite and one sandstone samples with #100 surfaces were used; 32 sliding angles for granite and 23 sliding angles for sandstone were measured without cleaning the surfaces. The sliding surfaces were re-polished after each test. Polishing and measuring procedures were repeated three times.

The sliding angles of the granite samples ranged from 41.6° to 23.3° (Fig. 13a). The average slip angles were distributed in a narrow range of 29.4° – 28.5° , within 1° of the basic friction angle. The first sliding angle appeared to decrease as the tilting speed increased, but the average of the measurements was almost the same regardless of the tilting speed. In the sandstone samples, the sliding angles ranged from 47.3° to 26.6° with similar ranges regardless of the tilting speed (Fig. 13b). The average sliding angles were within a narrow range of 32.8° – 34.0° , which is very close to the basic friction angle of sandstone. These results suggest that the tilting speed does not affect the sliding angle when the tilting speeds are within the range of 0.2 – $1.6^\circ/s$.

4.2.2 Effect of Sample Size

Four block sample sizes having a height (h) of 2 cm and a surface of 4×4 , 6×6 , 8×8 , and 10×10 cm were prepared to examine the influence of the sample size on the sliding angle. One granite and one sandstone samples with #100 surfaces were used. Thirty-two sliding angles were measured for the granite sample and 23 for the sandstone sample without cleaning the surfaces, following the procedure described in the above section. The surfaces were re-polished after each test. Polishing and measuring procedures were repeated three times.

Figure 14 shows the average, maximum, and minimum slip angles for the granite and sandstone samples with different sample sizes. The sliding angles for all the samples were always the highest at the first measurement and then

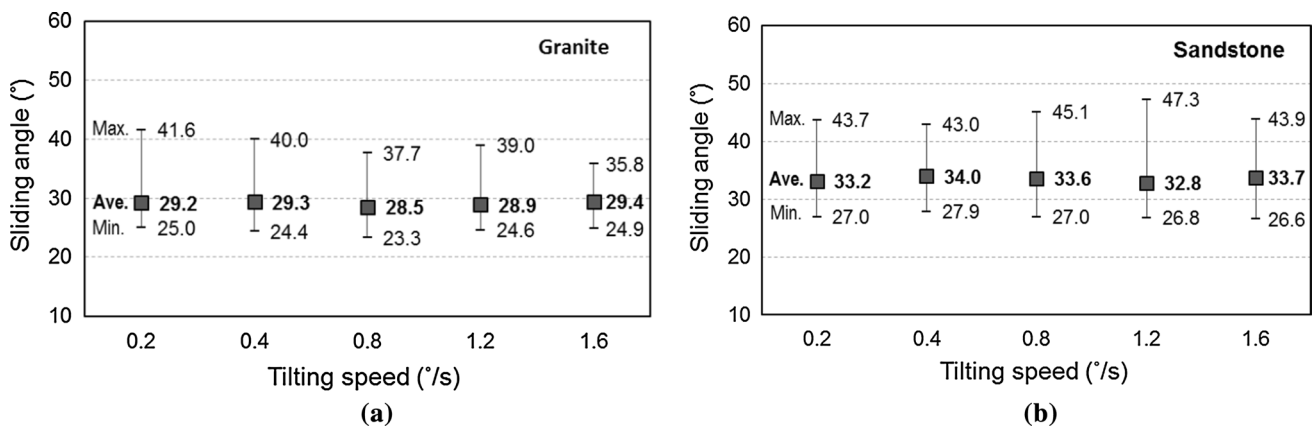


Fig. 13 Ranges and averages of sliding angles with different tilting speed for **a** granite (32 sliding angles) and **b** sandstone (23 sliding angles)

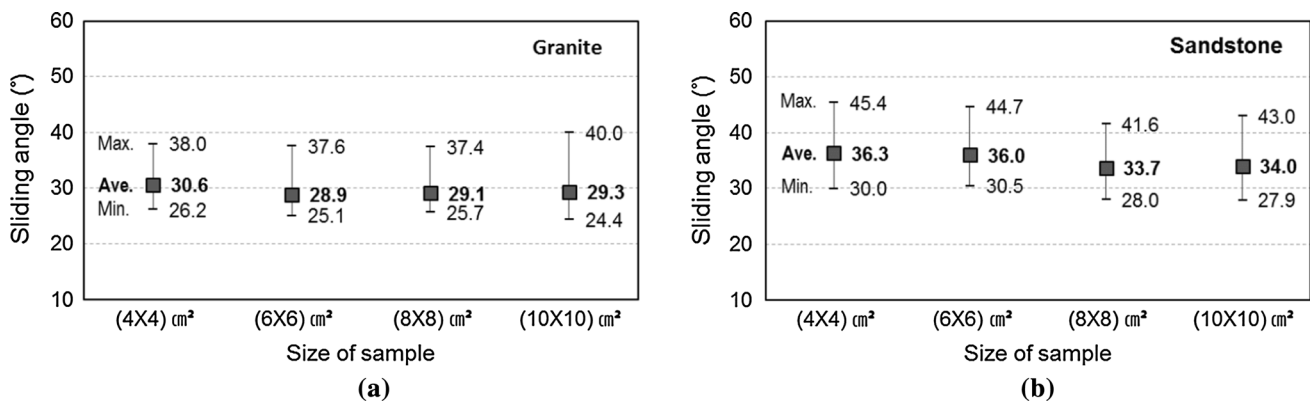


Fig. 14 Ranges and averages of sliding angles with different sample sizes for **a** granite (32 sliding angles) and **b** sandstone (23 sliding angles)

decreased exponentially as the measurements continued, in a similar trend to that shown in Figs. 11 and 12. Although the first and average sliding angles decreased slightly as the sample size increased for the sandstone samples, no such tendency was observed for the granite samples. The average sliding angles for the 4×4 cm granite samples and the 4×4 cm and 6×6 cm sandstone samples were slightly larger than the basic friction angle. The contact stress between sliding planes is compressive and tensile when sample is 4×4 cm, which is different from other samples (Fig. 2). These indicate that samples used in tilt tests should be larger than 8×8 cm for accurate measurements of the basic friction angle.

5 Summary and Conclusions

Surfaces were prepared from samples of Hwangdeung granite from Korea and Berea sandstone from the USA by saw-cutting or polishing using either #100 or #600 grinding powders. Their basic friction angles were then measured by direct shear tests, triaxial compression tests, and tilt tests.

The angles measured by direct shear tests on the #100 and #600 surfaces of granite were similar, yielding angles of 29.2° and 28.6° , respectively. However, the angle measured on the saw-cut surface was 25.5° , which is approximately 3° smaller than for the polished planes. The angles measured on the #100 surface and the saw-cut surface of the sandstone were similar, being 35.1° and 34.6° , respectively. The angle measured on the #600 surface was 26.4° , which is approximately 8° lower than that for the other surface types. The friction angle for the granite samples, as measured by triaxial compression tests, was 29.5° for the #100 surface, 28.8° for the #600 surface, and 25.2° for the saw-cut surface. The values from the triaxial tests for the sandstone were 33.1° for the #100 surface, 27.9° for the #600 surface, and 32.3° for the saw-cut surface. All the angles measured on the

#100 surface were similar, but those measured on the other surfaces varied with the measuring technique. Therefore, the basic friction angles were determined by averaging the values measured on the #100 surface, yielding 29.4° for the granite and 34.1° for the sandstone samples.

In the tilt test, the sliding angles were measured 50 times and the variation of the angles with testing conditions was investigated. Two surface conditions—surfaces cleaned and not cleaned after each tilt test—were used to examine the effect of the surface conditions on the friction angle. The first angles measured were approximately 40° regardless of rock type and surface conditions. This value is higher than the basic friction angle measured by the direct shear test and triaxial compression test. As the measurements continued for the polished surfaces the values tended to decrease exponentially. The angles measured on the 50th repetition were always lower than the basic friction angle measured in the other tests (direct shear and triaxial compression). The averages of the sliding angles from 50 measurements ranged from 27.6° to 19.1° for granite and from 31.0° to 21.9° for sandstone. When measured on the saw-cut surface, the sliding angles tended to increase or decrease linearly and differed from the basic friction angles; moreover, the differences between two adjacent measurements were large. Based on the characteristics of the sliding angles, the differences between the tilt tests, and the dispersion of the measurements in each test, it was concluded that in tilt tests the basic friction angle should be measured on the #100 surface which produced results similar to those of the direct shear test and triaxial compression test.

The averages of sliding angles at 10, 20, 30, 40, and 50 repetitions on the #100 surface were calculated. The smaller the number of measurements, the higher the average values are. For granite, the averages of 32 measurements without surface cleaning and 14 measurements with surface cleaning were very close to the basic granite friction angle. For sandstone, the average of 23 measurements without cleaning and

18 measurements with cleaning was the same as the basic sandstone friction angle. When 20–50 measurements without cleaning were averaged, the result for the basic friction angle was within $\pm 2^\circ$ for the granite and within $\pm 3^\circ$ for the sandstone samples. Sliding angles using five different tilting speeds were measured but the average angle was almost the same, indicating that tilting speed does not affect the sliding angle when tilting speeds are within the range of 0.2–1.6°/s. Sliding angles using four different sample sizes were also measured, resulting in a very accurate basic friction angle in the samples larger than 8×8 cm.

Acknowledgements This research is a basic research project funded by the Korean government (Ministry of Education) with the support of the Korea Research Foundation (NRF-2015R1D1A1A01056665).

References

- Alejano LR, González J, Muralha J (2012) Comparison of different techniques of tilt testing and basic friction angle variability assessment. *Rock Mech Rock Eng* 45(6):1023–1035
- Barton N (1973) Review of a new shear strength criterion for rock joints. *Eng Geol* 7:287–332
- Barton N (1976) The shear strength of rock and rock joints. *Int J Rock Mech Min Sci Geomech Abs* 13:255–279
- Barton N, Choubey V (1977) The shear strength of rock joints in theory and practice. *Rock Mech* 10(1–2):1–54
- Belem T, Homana-Etienne F, Souley M (2000) Quantitative parameters for rock joint surface roughness. *Rock Mech Rock Eng* 33(4):217–242
- Brace WF, Byerlee JD (1966) Stick-slip as a mechanism for earthquakes. *Science* 153:990–992
- Bridgman PW (1936) Shearing phenomena at high pressure of possible importance to geology. *J Geol* 44:653–669
- Bruce IG, Cruden DM, Eaton TM (1989) Use of a tilting table to determine the basic friction angle of hard rock samples. *Can Geotech J* 26:474–479
- Byerlee JD (1967) Frictional characteristics of granite under high confining pressure. *J Geophys Res* 72(14):3639–3648
- Coulson JH (1970) The effects of surface roughness on the shear strengths of joints in rock. Ph.D. thesis, University of Illinois, p 239
- Coulson JH (1972) Shear strength of flat surfaces in rock. In: Cording EJ (ed) 13th Symp rock mech, Am Soc Civil Eng, Urbana, pp 77–105
- Cruden DM, Hu XQ (1988) Basic friction angles of carbonate rocks from Kananaskis county, Canada. *Bull Int Assoc Eng Geol* 38(1):55–59
- Dehler W, Labuz JF (2007) Stress path testing of an anisotropic sandstone. *J Geotech Geoenviron Eng* 133(1):157–164
- Goldstein M, Goosev B, Pyrogovsky N, Tulinov R, Turovskaya A (1966) Investigation of mechanical properties of cracked rock. In: Proc of 1st ISRM congress, Lisbon, pp 521–524
- González J, González-Pastoriza N, Castro U, Alejano LR, Muralha J (2014) Considerations on the laboratory estimate of the basic friction angle of rock joints. In: Alejano R, Perucho A, Olalla C, Jimenez R (eds) *Rock eng and rock mech: structures in and on rock masses (EUROCK 2014)*, ISRM Eu Reg Symp, Vigo, pp 199–204
- Grasselli G, Egger P (2003) Constitutive law for the shear strength of rock joints based on three-dimensional surface parameters. *Int J Rock Mech Min Sci* 40(1):25–40
- Grasselli G, Wirth J, Egger P (2002) Quantitative three-dimensional description of a rough surface and parameter evolution with shearing. *Int J Rock Mech Min Sci* 39(6):789–800
- Hencher SR (1976) A simple sliding apparatus for the measurement of rock friction. *Discussion, Géotechnique* 26(4):641–644
- Hencher SR (2012) Discussion of Alejano, González and Muralha. *Rock Mech Rock Eng* 45:1137–1139
- Horn HM, Deere DU (1962) Frictional characteristics of minerals. *Géotechnique* 12:319–335
- Jaeger JC (1959) The frictional properties of joints in rock. *Geofisica Pura e Applicata* 43(1):148–158
- Jang HS, Jang BA (2015) New method for shear strength determination of unfilled, unweathered rock joint. *Rock Mech Rock Eng* 48(4):1515–1534
- Jang BA, Kim TH, Jang HS (2010) Characterization of the three dimensional roughness of rock joints and proposal of a modified shear strength criterion. *J Eng Geol* 20(3):319–327 (in Korean with English abstract)
- Krsmanovic D (1967) Initial and residual shear strength of hard rock. *Geotechnique* 17(2):145–160
- Krsmanovic D, Langof Z (1964) Large scale laboratory tests of the shear strength of rocky material. In: *Grundfragen auf dem Gebiete der Geomechanik/Principles in the Field of Geomechanics*, Springer Berlin Heidelberg, pp 2–30
- Kulatilake PHSW, Shou G, Huang TH, Morgan RM (1995) New peak shear strength criteria for anisotropic rock joints. *Int J Rock Mech Min Sci Geomech Abs* 32(7):673–697
- Ladanyi B, Archambault G (1969) Simulation of shear behaviour of a jointed rock mass. In: Proc 11th US symp on rock mech, Berkeley, ARMA-69-0105
- Lane KS, Heck WJ (1964) Triaxial testing for strength of rock joints. In: Proc 6th US symp on rock mech, Rolla, ARMA-64-098
- Lee SB, Chang CD (2015) Laboratory experimental study on fracture shear-activation induced by carbon dioxide injection. *J Geol Soc* 51(3):281–288 (in Korean with English abstract)
- Lee BH, Lee SJ, Choi SO (2014) A study on the relationship between basic frictional angle and mineral composition of granite sample. *Tunn Under Space* 24(1):32–45 (in Korean with English abstract)
- Maksimovic M (1992) New description of shear strength for rock joints. *Rock Mech Rock Eng* 25(4):275–284
- Muralha J (1995) Probabilistic approach of the mechanical behaviour of rock discontinuities. Ph.D. thesis, Instituto Superior Técnico, Lisbon (in Portuguese)
- Newland PL, Allely BH (1957) Volume changes in drained triaxial tests on granular materials. *Geotechnique* 7(1):17–34
- Papaliangas TT, Hencher SR, Lumsden AC (1995) A comprehensive peak shear strength criterion for rock joints. In: Proc 18th int cong rock mech, Tokyo, Japan, vol 1, pp 359–366
- Park JW, Song JJ (2013) Numerical method for the determination of contact areas of a rock joint under normal and shear loads. *Int J Rock Mech Min Sci* 58:8–22
- Patton FD (1966) Multiple modes of shear failure in rock and related material. Ph.D. thesis, University of Illinois, p 282
- Reeves MJ (1985) Rock surface roughness and frictional strength. *Int J Rock Mech Min Sci* 22(6):429–442
- Ruiz J, Li C (2014) Measurement of the basic friction angle of rock by three different tilt test methods. In: Alejano R, Perucho A, Olalla C, Jimenez R (eds) *Rock eng and rock mech: structures in and on rock masses (EUROCK 2014)*, ISRM EU reg symp, Vigo, pp 261–266

- Stimpson B (1981) A suggested technique for determining the basic friction angle of rock surface using core. *Int J Rock Mech Min Sci Geomech Abst* 18(1):63–65
- Wines DR, Lilly PA (2003) Estimates of rock joint shear strength in part of the Fimiston open pit operation in Western Australia. *Int J Rock Mech Min Sci* 40(6):929–937
- Yang ZY, Chiang DY (2000) An experimental study on the progressive shear behavior of rock joints with tooth-shaped asperities. *Int J Rock Mech Min Sci* 37(8):1247–1259